

# Membrane topology and site-specific mutagenesis of *Pseudomonas aeruginosa* porin OprD

Hongjin Huang,<sup>1</sup> Denis Jeanteur,<sup>2</sup> Franc Pattus<sup>3</sup> and Robert E. W. Hancock<sup>1\*</sup>

<sup>1</sup>Department of Microbiology, University of British Columbia, Vancouver, British Columbia, Canada V6T 1Z3.

<sup>2</sup>Protein Engineering Research Institute, 6-2-3 Furuedai, Suita, Osaka 565, Japan.

<sup>3</sup>Ecole Supérieure de Biotechnologie de Strasbourg, Pôle Universitaire d'Illkirch, 67400 Illkirch, France.

## Summary

*Pseudomonas aeruginosa* OprD is a 420-amino-acid protein that facilitates the uptake of basic amino acids, imipenem and gluconate across the outer membrane. OprD was the first specific porin that could be aligned with members of the non-specific porin superfamily. Utilizing multiple alignments in conjugation with structure predictions and amphipathicity calculations, an OprD-topology model was proposed. Sixteen  $\beta$ -strands were predicted, connected by short loops at the periplasmic side. The eight external loops were of variable length but tended to be much longer than the periplasmic ones. Polymerase chain reaction (PCR)-based site-specific mutagenesis was performed to delete separately short stretches (4–8 amino acid residues) from each of the predicted external loops. The mutants with deletions in the predicted external loops L1, L2, L5, L6, L7 and L8 were tolerated in both *Escherichia coli* and *P. aeruginosa*. The expressed mutant proteins maintained substantial resistance to trypsin treatment in the context of isolated outer membranes. Proteins with deletions in loops L1, L5, L6, L7 and L8 reconstituted similar imipenem supersusceptibility in a *P. aeruginosa* OprD:: $\Omega$  background. The L2-deletion mutant only partially reconstituted supersusceptibility, suggesting that loop L2 is involved in imipenem binding. These data were generally consistent with the topology model.

## Introduction

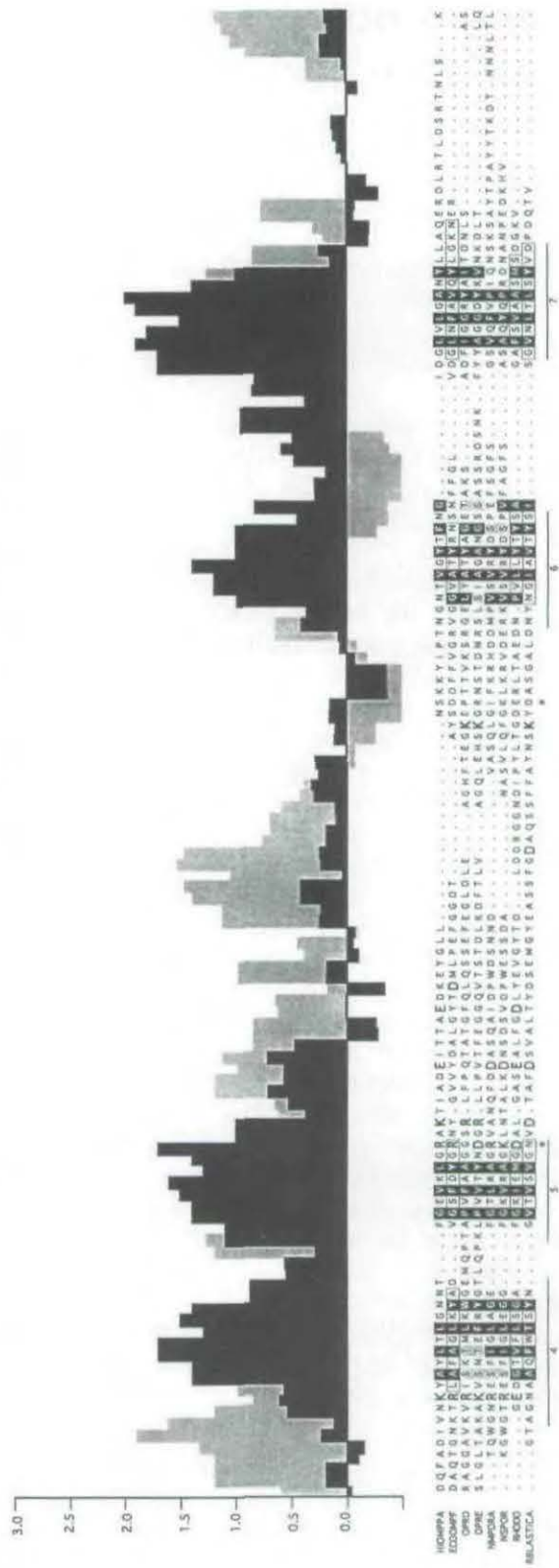
The porins of Gram-negative bacteria form water-filled

channels that permit the diffusion of hydrophilic solutes across the outer membrane (Hancock, 1987). They can be divided into two classes: (i) non-specific porins, which form channels that permit the general diffusion of hydrophilic molecules below a certain size and, therefore, are responsible for the exclusion limit of the outer membrane; and (ii) substrate-specific porins, which can facilitate the diffusion of specific substrates by virtue of having a specific substrate-binding site in their channel (Hancock, 1987). *Pseudomonas aeruginosa* outer-membrane protein, OprD, is a specific porin for basic amino acids, small peptides containing these amino acids and their structural analogue, the  $\beta$ -lactam antibiotic imipenem (Trias and Nikaido, 1990a,b). Competition experiments confirmed that basic amino acids and imipenem shared common binding sites within the OprD channel (Fukuoka *et al.*, 1991).

To fully understand the molecular mechanism involved in the facilitated uptake of basic amino acids and imipenem, a detailed knowledge of the molecular structure of OprD is required. Porins generally consist of transmembrane segments connected by turns and loops; a first approach to structure prediction was to identify turns (Paul and Rosenbusch, 1985). Another approach was based on the assumption that transmembrane strands are amphipathic, with one face being in contact with the hydrophobic core of the lipid and other facing the pore lumen (Vogel and Jahnig, 1986). By combining the prediction of topology with multiple alignments of a set of porin sequences from distantly related species, Jeanteur *et al.* (1991; 1994) greatly improved the quality of these predictions. The general relevance of this method was confirmed by the crystal structures of OmpF, PhoE and *Rhodobacter capsulatus* porins (Cowan *et al.*, 1992; Weiss and Schulz, 1992).

For most porins, in the absence of precise crystallographic data, genetic, immunological and biochemical approaches have been employed to test the accuracy of predicted structures. Gene-fusion techniques using  $\beta$ -galactosidase, alkaline phosphatase and  $\beta$ -lactamase as reporter enzymes were successful in studies of the folding of inner-membrane proteins, which contain transmembrane segments composed of hydrophobic residues forming  $\alpha$ -helices (Manoil and Beckwith, 1986). However, such techniques have not proved to be suitable for the study of outer-membrane protein topology. Another technique,

Received 8 August, 1994; revised 30 January, 1995; accepted 3 February, 1995. \*For correspondence. E-mail Bob@CBDN.CA; Tel. (604) 822 3489; Fax (604) 822 6041.





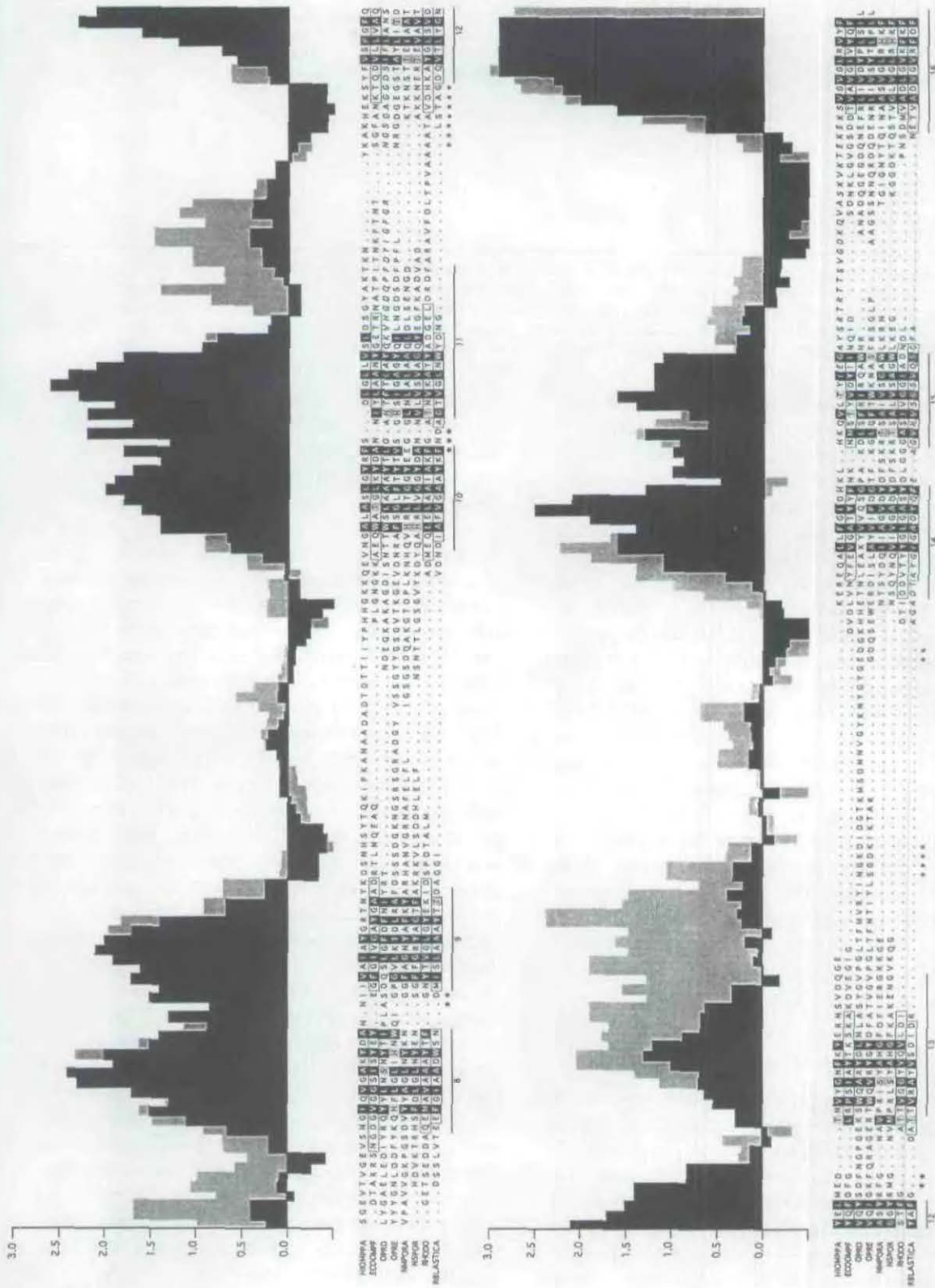


Fig. 1. Alignment of the porin sequence representatives of the porin superfamily together with OprD and OprE sequences. Membrane-spanning strands for the structurally defined porins are boxed. The lines and numbers under the alignment represent the predicted  $\beta$ -strands. The residues which were predicted to face the hydrophobic core of the membrane are shaded; some of them presenting certain polar properties are lightly shaded. Aromatic residues are shown in bold, charged residues involved in the eyelet are bold and are bigger in size. Major turn predictions are indicated by asterisks. The membrane criterion ( $\bar{n} + \langle \mu \rangle$ ) calculated for 32 sequences (Jeanneau *et al.*, 1994) is shown in black, with values shown on the y axis. The hydrophobic moment was calculated using a periodicity of 1/2 and 1/2.5 in order to take into account untwisted and twisted  $\beta$ -strands. Each column represents a ( $\bar{n} + \langle \mu \rangle$ ) calculated with a window of nine residues centred at the current position. The calculation for the OprD sequence alone is displayed in grey.

**Table 1.** Homologies and identities among the porin superfamily.

| Identities     | HIOMPPA<br><i>H. influenzae</i><br>P2 | ECOOMPF<br><i>E. coli</i><br>OmpF | OPRD<br><i>P. aeruginosa</i><br>OprD | OPRE<br><i>P. aeruginosa</i><br>OprE | NMPORA<br><i>N. meningitidis</i><br>PorA1 | NSPOR<br><i>N. scca</i><br>Por | RHODO<br><i>R. capsulatus</i><br>P312443 | RBLASTICA<br><i>R. blastica</i> |
|----------------|---------------------------------------|-----------------------------------|--------------------------------------|--------------------------------------|---|--------------------------------|--|---------------------------------|
| Homologies (%) | M93268                                | M74489                            | Z14065                               | P32722                               | X52995                                    | X65461                         |  |                                 |
| HIOMPPA        |                                       | 21                                | 9                                    | 8                                    | 17  | 15                             | 14                                       | 15                              |
| ECOOMPF        | 30                                    |                                   | 15                                   | 12                                   | 16  | 21                             | 18                                       | 16                              |
| OPRD           | 18                                    | 23                                |                                      | 39                                   | 13  | 11                             | 11                                       | 11                              |
| OPRE           | 15                                    | 20                                | 51                                   |                                      | 11  | 11                             | 11                                       | 10                              |
| NMPORA         | 27                                    | 26                                | 22                                   | 22                                   |   | 47                             | 16                                       | 13                              |
| NSPOR          | 26                                    | 32                                | 21                                   | 21                                   | 58  |                                | 15                                       | 13                              |
| RHODO          | 26                                    | 28                                | 19                                   | 18                                   | 27  | 26                             |  | 28                              |
| RBLASTICA      | 25                                    | 26                                | 18                                   | 17                                   | 24  | 25                             | 40                                       |                                 |

Aligned sequences were analysed with DISTANCE (Devereux *et al.*, 1984) using a threshold of 1.0 for identities and 0.6 for homologies. Identities between sequences are shown on the top part of the table while homologies are at the bottom. The headings at the top give, together with the name of the alignment, the species, gene name and accession number. Accession number beginning with the letter P are from the SWISSPROT database and others are from the GenBank/EMBL database. Where accession numbers are provided, the sequence and gene name correspond to that entry. RBLASTICA was typed by hand from the original reference (Kreusch *et al.*, 1994).

linker insertion mutagenesis, involving introduction of a short stretch of amino acids, modifies the protein in a more subtle way. It has been successfully used to study the topology of several *Escherichia coli* porins, including LamB (Boulain *et al.*, 1986) and PhoE (Bosch and Tommassen, 1987), and *P. aeruginosa* OprF (Wong *et al.*, 1993). In addition, limited deletion studies have been performed on loops 4 and 5 of PhoE (Agterberg *et al.*, 1989) and loop 3 of OmpF (Benson *et al.*, 1988) and OmpC (Misra and Benson, 1988). Such studies, and the above-mentioned multiple alignments of porin sequences, suggest that the regions that can accept the insertion or deletion of varying lengths of amino acids are largely located in the loop regions that interconnect the  $\beta$ -strands of porins. Therefore, we have modified existing methods to develop an efficient site-specific deletion mutagenesis technique.

In this study, we present the first OprD topology model constructed by utilizing multiple alignment together with the secondary structure predictions. Polymerase chain reaction (PCR)-mediated, site-specific mutagenesis was then employed to delete separately the predicted external loops and to permit confirmation of the general accuracy of the model.

## Results

### Prediction of the OprD topology model

In a previous paper (Jeanteur *et al.*, 1994), the alignments of 30 non-specific porins from five distant families were reported. Alignment of OprD was not considered in detail. However, attempts to match the OprD sequence with other *P. aeruginosa* porins and the *E. coli* porins OmpF and TolC showed that OprD had the highest homology to OmpF, with an alignment score, using the Needleman and Wunsch method (1970) of 2.6. This is close to 3.0, the minimal score required for an alignment to be considered significant (Huang *et al.*, 1992). Although

OprD was a specific porin for basic amino acids and imipenem, in contrast to other members of the non-specific porin superfamily its alignment to OmpF was almost as good as that of OmpF to the structurally related (Cowan *et al.*, 1992; Weiss and Schulz, 1992) porin from *R. capsulatus* (Table 1). In contrast, we were unsuccessful in aligning other specific porins such as *E. coli* porin LamB or Tsx with members of the porin superfamily. The detailed examination described here demonstrates that alignment is stronger in the predicted membrane-spanning regions and, on this basis, OprD is the first specific porin that can be included in the porin superfamily alignment (Fig. 1).

Sixteen  $\beta$ -strands were predicted and could be aligned to those of other members of the porin superfamily (Fig. 1). Alignment was very clear for the N- and C-terminal  $\beta$ -strands, but the homology was weaker in the middle part of the sequence, a result similar to that reported for other porins (Jeanteur *et al.*, 1991). Four other segments, according to our membrane criteria, could also be predicted as transmembrane segments but were rejected in the alignment procedure. In addition, the placement of  $\beta$ -strands 7 and 8 relied on the fact that an alternative placement led to creation of a short loop 4, which when deleted as described below, did not result in expression. The ambiguous placement of strand 13 was resolved to minimize the length of the periplasmic turn between  $\beta$ -strands 12 and 13 in the final model. The 16 transmembrane segments had the typical amphipathic features of porin  $\beta$ -strands in that they were composed of alternating polar and non-polar residues exposed to the aqueous channel and hydrophobic membrane interior, respectively (Fig. 2). The sizes of the predicted  $\beta$ -strands (9–16 residues) were in agreement with the lengths of  $\beta$ -strands observed for the solved porin structures, and the ends of these  $\beta$ -strands were often composed of aromatic residues, which may function as one of the stabilizing forces for the  $\beta$ -barrel structure (Cowan *et al.*, 1992).



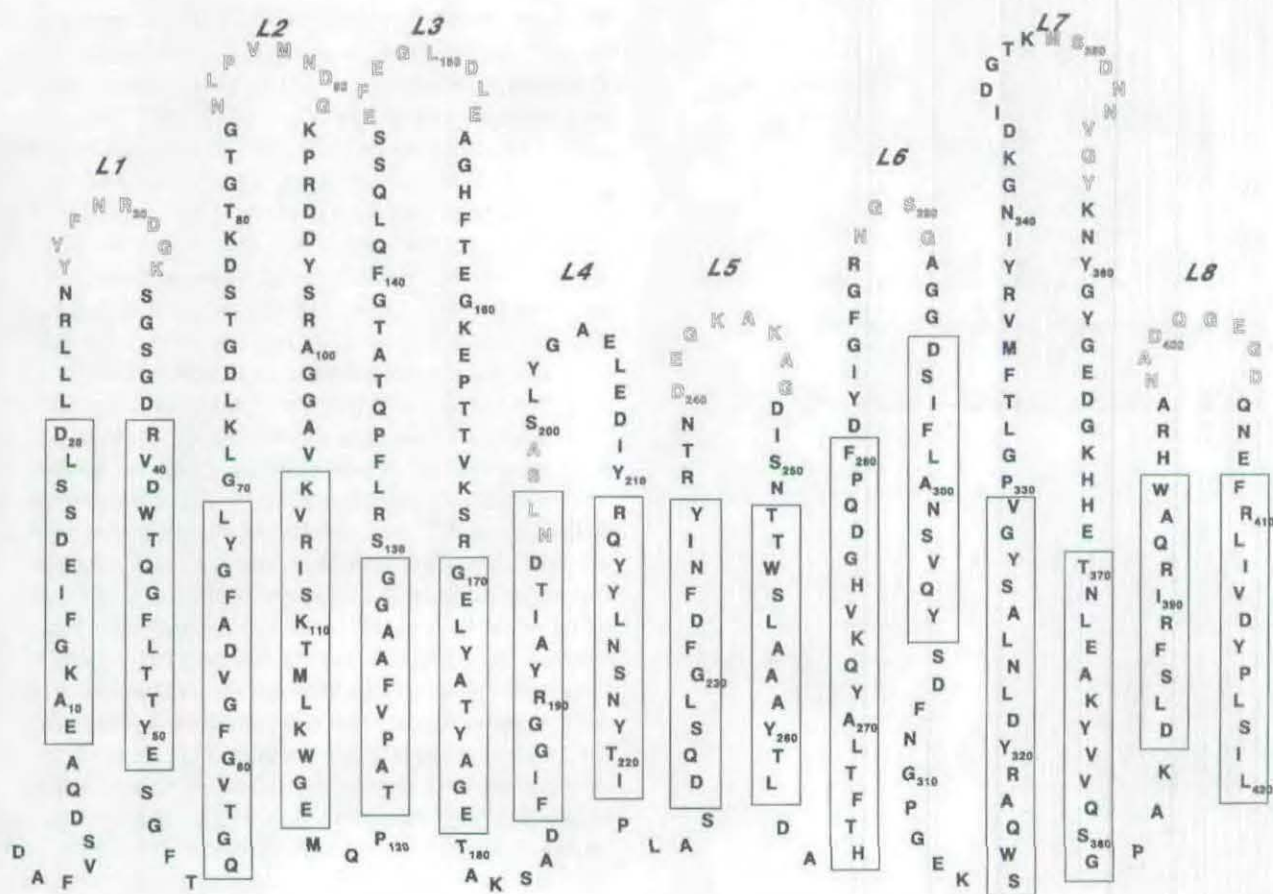


Fig. 2. Proposed membrane topology of OprD. The 16 predicted transmembrane  $\beta$ -strands are boxed, and the eight external loops are labelled as L1 to L8. The deleted amino acid residues are presented as unfilled letters.

Four periplasmic turns, T1, T4, T5 and T6, were clearly predicted by turn propensity analysis (Fig. 1). T3 was also detected by this analysis but less clearly. Most of these turns were short (2–9 residues) and of about the same length as those determined from the known structures.

Consistent with the larger number of amino acids in OprD than in the other members of the porin superfamily, the eight external loops were often slightly longer than the ones observed for the known porin structures. The predicted loop 3 (S-130 to R-169) was as long or longer than any other loops (Fig. 2). It was also the longest external loop observed in the crystal structures of *E. coli* OmpF and PhoE, and *R. capsulatus* and *Rhodospseudomonas blastica* porins, in which it folded inside the pore forming the constriction of the pore (Cowan *et al.*, 1992; Weiss and Schulz, 1992; Kreuzsch *et al.*, 1994).

#### PCR-mediated site-specific deletion mutagenesis

To test the validity of the predicted external loops, site-specific deletion mutagenesis was performed to delete, separately, short stretches of amino acids (4–8) from

each predicted loop to see if these deletions were tolerated or not. With one exception, the deletions were made around the middle of the predicted loops, as shown by the unfilled letters in Fig. 2. The exception was loop L4, for which the original prediction was apparently erroneous.

Early methods for site-directed mutagenesis using single-stranded DNA gave low efficiencies of obtaining the desired mutation. The development of PCR (Saiki *et al.*, 1985), however, provided a new approach (Vallette *et al.*, 1989), in which primers bearing the mutations are incorporated into the PCR products. In this work, two PCR strategies, direct extension (loops L1, L3, L6 and L7) and overlap extension (loops L2, L4, L5 and L8), were used. The strategies for PCR were optimized to obtain a high rate (around 90%) of successful mutagenesis. From the mutagenesis of each predicted loop, five mutant plasmids containing the deletions were selected and the whole PCR-amplified regions were sequenced.

#### Characterization of the deletion mutants

The mutant plasmids pHE1 to pHE8, corresponding to the

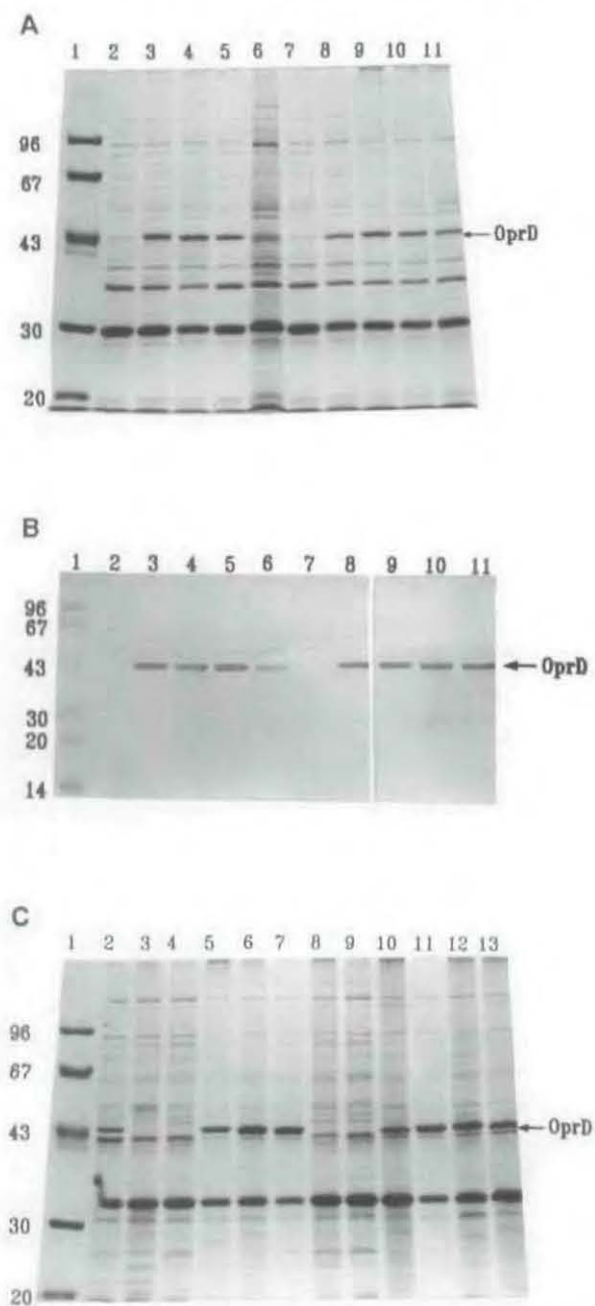


**Fig. 3.** SDS-PAGE (A) and Western immunoblot (B) demonstrating the expression of OprD derivatives in the outer membrane of *E. coli* CE1248. The banding position of OprD is indicated by an arrow on the right. Lane 1 contained molecular weight markers. Lanes 2–11 contained outer membranes from CE1248 with the following plasmids: lane 2, pMTZ19R; lane 3, pMBK19R; lane 4, pHE1; lane 5, pHE2; lane 6, pHE3; lane 7, pHE4; lane 8, pHE5; lane 9, pHE6; lane 10, pHE7; and lane 11, pHE8. For each lane, 20  $\mu$ g outer membrane protein was loaded. C. The expression of OprD derivatives in the outer membrane of *P. aeruginosa* OprD-defective strain H729. The banding position of OprD is indicated by an arrow on the right. Lane 1, molecular weight marker; lane 2, H103; lane 3, H729. Lanes 4–11 contained outer membranes from H729 containing the following plasmids: lane 4, pUCP19, lane 5, pXH2; lane 6, pHP1; lane 7, pHP2; lane 8, pHP3; lane 9, pHP4; lane 10, pHP5; lane 11, pHP6; lane 12, pHP7; lane 13, pHP8. For each lane, 20  $\mu$ g outer membrane protein was loaded.

deletions on the predicted loops L1 to L8, were transformed into the porin-deficient *E. coli* strain CE 1248. The outer membranes containing the deletion mutations were isolated and examined by SDS-PAGE (Fig. 3A), and on Western immunoblots using an anti-OprD polyclonal antiserum (Fig. 3B). The mutant polypeptides from the deletion mutagenesis of six predicted loops, L1, L2, L5, L6, L7 and L8, co-fractionated with the outer membranes, were typically heat modifiable and were expressed at similar levels compared with cells expressing wild-type OprD (Fig. 3A, lanes 4, 5, 8–11). They also showed a slightly increased electrophoretic mobility as compared with wild-type OprD, consistent with the deletion of a few amino acid residues. These results indicated that deletions of short stretches of amino acids in these six predicted loops did not substantially change the native conformation of OprD, and that the consequent mutant proteins were assembled into the outer membrane, a result suggesting that these loops were accurately predicted. The deletion of the predicted loop L3 caused diminished but observable expression (Fig. 3A, lane 6), as confirmed by Western immunoblot results (Fig. 3B, lane 6), indicating that this deletion was tolerated. However, since the deleted stretch had four negatively charged residues (Fig. 2), which could be important for protein folding, the deletion may have perturbed the OprD structure sufficiently to lead to reduced protein production or unstable products. The deletion of the originally predicted loop L4 did not permit stable expression of an OprD protein (Fig. 3, lane 7). The deletion may have involved a transmembrane segment or a much less flexible turn, which led to a modification of our first model.

To permit functional studies, the expression of these OprD derivatives was examined in the native host *P. aeruginosa*. All of the mutant *oprD* genes were subcloned in the same orientation as the *lac* promoter into the shuttle plasmid pUCP19 (Schweizer, 1991). The recombinant plasmids, pHP1 to pHP8, corresponding to the deletions of the predicted loops L1 to L8, respectively, were then transformed into the *P. aeruginosa* OprD-defective strain H729. Examination of plasmid-encoded  $\beta$ -lactamase levels indicated no significant difference ( $p > 0.5$ ) in  $\beta$ -lactamase levels for any of the transformants, suggesting that the plasmids were present in similar copy numbers (Table 2). SDS-PAGE (Fig. 3C), as confirmed by Western-immunoblot analysis, showed the same profile as that observed in *E. coli*, with the exception of the mutant deleting eight residues of predicted loop L3, for which no expression was observed (Fig. 3C, lane 8). This further confirmed that six of the predicted loops were accurate. The loop L3 mutant grew much slower than the remaining mutants.

#### *Trypsin susceptibility of the deletion variants*

The above results indicated that the OprD derivatives were



**Table 2.** Antibiotic susceptibilities of *P. aeruginosa* OprD mutant strains.

| Strain       | Beta-lactamase activity <sup>a</sup> | MICs ( $\mu\text{g ml}^{-1}$ ) |           |            |           |
|--------------|--------------------------------------|--------------------------------|-----------|------------|-----------|
|              |                                      | imipenem                       | meropenem | gentamicin | polymyxin |
| H729         | 5.4 $\pm$ 0.6                        | 16.0                           | 2.0       | 2.0        | 4.0       |
| H729(pUCP19) | 166 $\pm$ 15                         | 16.0                           | 2.0       | 1.0        | 4.0       |
| H729(pXH2)   | 194 $\pm$ 53                         | 0.5                            | 0.125     | 2.0        | 4.0       |
| H729(pHP1)   | 129 $\pm$ 44                         | 1.0                            | 0.125     | 1.0        | 4.0       |
| H729(pHP2)   | 128 $\pm$ 26                         | 4.0                            | 1.0       | 2.0        | 2.0       |
| H729(pHP5)   | 122 $\pm$ 21                         | 1.0                            | 0.125     | 1.0        | 4.0       |
| H729(pHP6)   | 188 $\pm$ 56                         | 1.0                            | 0.06      | 2.0        | 2.0       |
| H729(pHP7)   | 135 $\pm$ 26                         | 0.5                            | 0.06      | 2.0        | 4.0       |
| H729(pHP8)   | 131 $\pm$ 35                         | 0.5                            | 0.06      | 2.0        | 4.0       |

a. Activity in nmol nitrocefin  $\text{mg}^{-1}$  cells  $\text{min}^{-1}$ .

properly located and assembled in the outer membrane. To probe the configuration of these OprD derivatives in *P. aeruginosa*, trypsin-susceptibility assays were performed.

Outer membrane proteins tend to be protease resistant because of their possession of extensive  $\beta$ -structures, with the linking surface loops tightly packed and folded in towards the porin channel (Cowan *et al.*, 1992). In our studies, trypsin treatment of the outer membrane from H729 containing wild-type OprD protein resulted in substantial retention of the full-size OprD with a small amount of degradation to two protected fragments of apparent molecular masses of 32 kDa and 16 kDa (Fig. 4, lane 3). Similar results were obtained for *P. aeruginosa* strain H729 expressing OprD derivatives with deletions in loops L7 and L8 (Fig. 4, lanes 8, 9). Derivatives with deletions in loops L1, L2, L5 and L6 also were substantially trypsin resistant, although one or two additional fragments of mass 25 kDa and 40 kDa were generated by trypsin treatment (Fig. 4, lanes 4–7). This agrees with the proposal that deletions of these predicted loops could cause local modifications of OprD configuration, leading to the exposure of certain trypsin-susceptible sites. Nevertheless, these data are generally consistent with the correct folding of the OprD derivatives. Increasing the amounts of trypsin and/or incubation time resulted in the generation of more fragments for both wild-type and mutant OprD.

#### Functional studies

To further confirm that the conformations of OprD derivatives were not extensively changed with respect to native OprD and to see if any of the deletions influenced the function of OprD as a channel for imipenem and the related carbapenem antibiotic meropenem, MICs were assessed for those two antibiotics in the OprD-defective strain H729 background. As previously demonstrated (Huang and Hancock, 1993), strain H729 expressing excess OprD from plasmid pXH2 had an MIC that was 16–32-fold lower than those observed for strain H729 and H729 carrying the vector pUCP19 (Table 2). Similarly, there was a

16–32-fold reduction in MIC for strain H729 expressing the mutant OprDs with deletions in loops L1, L5, L6, L7 or L8. In contrast, the loop L2 deletion expressed from plasmid pHP2 resulted in only a 2–4-fold reduction in MIC to imipenem and meropenem (Table 2, Fig. 5). Control antibiotics gentamicin and polymyxin demonstrated no significant difference in MIC for any of the strains studied (note that a twofold difference in MIC is considered by convention to be within experimental variability), indicating that the mutant proteins did not cause gross outer-membrane distortions.

It has been previously demonstrated that lysine will compete with imipenem for uptake through OprD (Fukuoka *et al.*, 1991; Huang and Hancock, 1993), resulting in an increasing MIC as a function of lysine concentration. In contrast, lysine had no significant effect on imipenem MICs measured using the loop 2 deletion mutant OprD strain H729(pHP2) (Fig. 5). These data suggest that this deletion substantially influences the passage of both imipenem and lysine through OprD.

#### Discussion

We have presented here a prediction for the topology of OprD and an approach to assess the general accuracy



**Fig. 4.** Western immunoblot of trypsinized outer membrane samples of *P. aeruginosa* strain H729 containing OprD derivatives. Lane 1, molecular weight marker; lane 2, untreated wild-type OprD control; lanes 3–9, trypsin-treated outer membranes from H729 with the following plasmids: lane 3, pXH2; lane 4, pHP1; lane 5, pHP2; lane 6, pHP5; lane 7, pHP6; lane 8, pHP7; and lane 9, pHP8.



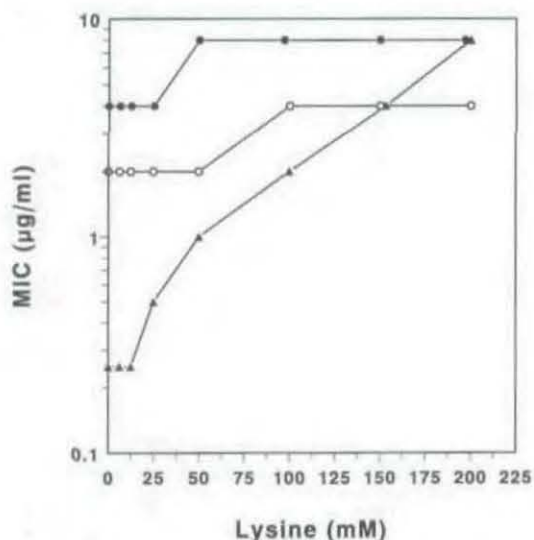


Fig. 5. Effect of varying lysine concentrations on the MICs of imipenem for the *oprD*:: $\Omega$  mutant H729 complemented with the vector control pUCP19 (●), the loop 2 deletion mutant plasmid pHP2 (○) and the unaltered *OprD* gene in plasmid pXH2 (▲).

of this model. Eight *OprD* variants were constructed by deleting 4–8 amino acids from each of the predicted external loops. Six of these deletion variants were well tolerated both in *E. coli* and *P. aeruginosa*, one was tolerated only in *E. coli* and one did not give rise to protein expression in *E. coli* or *P. aeruginosa*.

Previous studies have indicated that *OprD* has specific binding sites for basic amino acids and imipenem, but no work has been done to identify the structural characteristics of this porin or the specific binding sites which are involved in antibiotic and nutrient uptake through this specific channel. In the absence of crystallographic data, we chose to attempt to predict an *OprD* topology model. It must be stated, however, that such methods do not permit an accurate prediction of the exact amino acids at which  $\beta$ -strands and loop regions start and finish.

The published crystal structures of the *E. coli* porins *OmpF* and *PhoE*, and the *R. capsulatus* and *R. blastica* porins, revealed trimers of identical subunits. Each monomer subunit consisted of 16 anti-parallel  $\beta$ -strands forming a barrel surrounding a pore. These strands are connected by very short loops on the periplasmic face of the porin, whereas the loops on the outside of the bacteria are of variable length but in general are longer (Cowan *et al.*, 1992; Weiss and Schulz, 1992; Kreusch *et al.*, 1994). Analysing the structure of a family of bacterial porins by sequence alignment and structure predictions suggested similar structures for all bacterial porins in the porin superfamily (Jeanteur *et al.*, 1991). However, *P. aeruginosa* *OprD*, like other specific porins, was considered unlikely to align with the porin superfamily. In contrast, we demonstrate here that a combination of multiple alignments and

prediction of amphipathic  $\beta$ -strands using membrane criteria permitted a reasonable alignment between *OprD* and the porin superfamily (Fig. 1). Deletion mutagenesis subsequently provided evidence in support of our topology model.

Porins have been subdivided into two classes: specific porins and general porins (Hancock, 1987). *R. capsulatus* porin has been classified as a general porin. However, in the crystal structure, a solute-binding site was observed within the pore close to the eyelet, with an unknown solute co-crystallized in it (Weiss and Schulz, 1992). Furthermore, this porin has been reported to bind efficiently to tetrapyrroles (Bollivar and Bauer, 1992). Therefore, the *R. capsulatus* porin that had been previously assigned to the class of general porins may actually be both specific and non-specific, depending on the solute. Based on this observation, Schulz (1994) first proposed that many porins belong to both classes, but that the specific substrates have been detected in only a few porins. Consistent with this, *E. coli* sucrose porin *ScrY* had the functional characteristics of both a general diffusion pore and a substrate-specific pore (Schulein *et al.*, 1991). We also observed that *OprD* could facilitate the uptake of gluconate under the growth rate-limiting conditions (Huang and Hancock, 1993). Competition experiments indicated no common binding sites were shared between gluconate and basic amino acids. One possible explanation is that *OprD* is a specific porin for basic amino acids, but that it may also function as a general porin for small substrates such as gluconate. The alignment of *OprD* with the porin superfamily provides strong evidence to support Schulz's proposal about the dual nature of certain porins.

The *OprD* model provided a prediction of the flexible segments (loops) of *OprD*. Generally speaking, insertions or deletions in porins should be non-disruptive only if they occur in the surface loops. Consistent with this, sequence comparisons of porins from distant families showed that the loop regions often varied substantially in length, in contrast to the highly conserved  $\beta$ -strands (Jeanteur *et al.*, 1994). One reason is that selective pressure from the environment, e.g. antibiotics or phages, may play a role in forcing certain regions to evolve at a higher rate than others. Another possible explanation is that the external loops simply have more freedom to change without altering porin secretion, folding and function. For example, deletions of certain *PhoE* cell surface-exposed regions did not interfere with the translocation across the inner membrane or the incorporation into the outer membrane (Agterberg *et al.*, 1989). Moreover, spontaneous deletions located in the *OmpF* or *OmpC* external loops could produce *OmpF* or *OmpC* proteins which were active and allowed the passage of large maltodextrins (Benson *et al.*, 1988; Misra and Benson, 1988). In contrast, the membrane-spanning segments contribute especially to



the conformation required for stability, folding or outer membrane localization, since studies involving deletion mutagenesis of PhoE, removing either the first (Bosch *et al.*, 1988) or the last (Bosch *et al.*, 1989) transmembrane segment, drastically affected or completely inhibited incorporation into the outer membrane.

Three criteria were used to evaluate whether the mutant proteins folded into near-native configurations. First, the polypeptides encoded by mutant OprD alleles in *E. coli* and the native host *P. aeruginosa* were identified. The high levels of expression and correct location in the outer membrane of OprD derivatives containing deletions of the presumed loops L1, L2 and L5 to L8 were consistent with our model. The deletion of predicted L3 was tolerated in *E. coli* but resulted in reduced expression. The same phenomenon was observed for certain deletion mutants of PhoE (Agterberg *et al.*, 1989). The L3 deletion mutant did not direct the production of any OprD in the outer membrane of *P. aeruginosa*. This may reflect an innate and more efficient ability of *P. aeruginosa* to proteolyse unstable products. A second criterion used to assess configuration was trypsin susceptibility. All of the OprD derivatives were resistant to digestion to some extent, indicating that the deletions did not cause extensive alterations in configuration. The third criterion was functional activity. All of the tolerated deletion mutant OprDs could form functional channels and did not grossly disrupt the outer membrane, which retained its barrier properties against polymyxin and gentamicin. Five of the deletion mutants could reconstitute imipenem and meropenem susceptibility. Only one, the loop 2 deletion mutant, had lost the ability to reconstitute full susceptibility, suggesting a possible role for loop L2 in imipenem binding. Our data, however, do not preclude the co-involvement of loop L3, which, in the structurally defined members of the porin superfamily, folds into the centre of the channel to form the 'eyelet' region determining channel diameter and selectivity.

## Experimental procedures

### Bacterial strains, plasmids and growth conditions

*P. aeruginosa* PAO1 strain H103 was used as the OprD-containing wild-type strain (Woodruff and Hancock, 1988). *P. aeruginosa* H729 was an *oprD::Ω* derivative of strain H103 created by gene replacement with a kanamycin-resistant  $\Omega$  interposon-mutated *oprD* gene (Huang and Hancock, 1993). *E. coli* DH5 $\alpha$  F' (F' *endA1 hsdR17* ( $r_{\text{K}}$   $m_{\text{K}}$ ) *supE44 thi-1 recA1 gyrA96 relA1*  $\lambda^{-}$   $\Phi$ 80d*lacZΔM15 Δ(lacZYA argF) U169*) was used for primary cloning (Sambrook *et al.*, 1989). *E. coli* CE1248 (F' *recA56 phoE proA,B phoR69 omp-B471 thr leu thi pyrF thy ilvA his lacY argG tonA rpsL cod dra utr glpR*) (van der Ley *et al.*, 1985) was a strain with mutations preventing the production of porins OmpF, OmpC and PhoE.

Plasmid pBK19R contained the *oprD* gene which was

cloned as the 2.1 kb *Bam*HI–*Kpn*I fragment into pTZ19R in the same orientation as the *lac* promoter (Huang *et al.*, 1992). Broad-host-range plasmid pUCP19 (Schweizer, 1992) was used for the overexpression of OprD in *P. aeruginosa*.

Strains were routinely grown on Luria broth (LB) medium (1.0% Bacto Tryptone, 0.5% yeast extract, 0.5% NaCl) or LB agar containing, in addition, 2% Bacto agar. *P. aeruginosa* strains were also grown on Mueller–Hinton broth. Antibiotics were used in selective media at the following concentrations: ampicillin for *E. coli* (75  $\mu\text{g ml}^{-1}$ ) (replaced by 750  $\mu\text{g ml}^{-1}$  carbenicillin for *P. aeruginosa*); kanamycin, 35  $\mu\text{g ml}^{-1}$  for *E. coli*; 300  $\mu\text{g ml}^{-1}$  for *P. aeruginosa*.

### Prediction of the OprD topology model

According to Paul and Rosenbusch (1985), a turn could be defined as a segment consisting of three or more residues containing at least one 'turn promoter' and no 'turn blockers'. We refined this criterion by computing a frequency matrix of residue occurrence within short periplasmic turns, external loops and transmembrane strands from those porins with known structures (Cowan *et al.*, 1992; Weiss and Schulz, 1992) and from a set of very closely related porins. Using a linear matrix of turn frequencies, turns were predicted as segments of three residues with a 'turn promoter' propensity that was three times higher than the 'turn blocker' propensity.

The membrane criterion value, using a linear combination of hydrophobicity (Cornette *et al.*, 1987) and hydrophobic moment (Eisenberg *et al.*, 1982),  $\bar{h} + \langle \mu \rangle$ , was used to predict the transmembrane segments quite precisely (Jeanteur *et al.*, 1991).

Alignments of closely related sequences were performed using the classical alignment tools available in the GCG package (Devereux *et al.*, 1984). For distant sequences, such tools are not very accurate, mainly because they tend to introduce gaps which incur the same penalty all along the sequence. For porins, it is clear that the loop regions are much more variable and even very long gaps may be easily introduced without problems. Conversely, insertion of gaps in the transmembrane regions should be heavily penalized. Therefore this was taken into account manually in the final alignment predictions (Fig. 2).

In general, a  $\beta$ -strand was defined as a segment with a high value for the membrane criterion, no gaps, no turn predictions and sequence conservation. In contrast, a loop was defined by its low value of membrane criterion, the presence of gaps, turn predictions and sequence variability.

### Plasmid construction

Plasmid pMBK19R and pMBE19R were derivatives of pBK19R and constructed as follows. Plasmid pTZ19R was digested by *Sal*I and *Hind*III, and the consequent fragment was blunt ended by Klenow fragment and then self-ligated to form plasmid pMTZ19R. This procedure eliminated the restriction sites *Sal*I, *Pst*I, *Sph*I and *Hind*III in the multiple cloning site. The 2.1 kb *Bam*HI–*Kpn*I fragment from pBK19R containing the *oprD* gene was cloned into pMTZ19R to form pMBK19R, which was used as the template for the mutagenesis of the predicted loops L3 to L8 of OprD. The 1.2 kb *Bam*HI–*Eco*RI fragment from pBK19R containing the



N-terminal coding region of the *oprD* gene was cloned into pMTZ19R to construct pMBE19R, which was used as the template for the deletion mutagenesis of predicted loops L1 and L2.

#### PCR-mediated site-specific deletion mutagenesis

Two strategies were used for this purpose. Strategy I, direct extension (Vallette *et al.*, 1989), was applied to those loop-encoding regions with convenient restriction sites adjacent to the desired deletion nucleotide sequence. For those loop-encoding regions without convenient restriction sites located near the sites of mutagenesis, strategy II, overlap extension (Ho *et al.*, 1989), was employed. The amplified DNA was cleaved with the appropriate restriction enzymes and cloned back into the parental plasmid that had been cleaved with the same pair of restriction enzymes.

To design primers, the PCGENE program was used to minimize the chance of non-specific binding and primer-dimer interactions. For the mutagenic primers, at least 20 nucleotides from each side of the deletion site were included. Oligonucleotide primers were synthesized on an Applied Biosystems Incorporated Mode 392 DNA/RNA synthesizer. The actual primer sequences utilized are available from the authors on request. Oligonucleotides were purified by C<sub>18</sub> SEP-PAK (Millipore Co.) according to the manufacturer's protocol.

The PCR reaction mixture (total volume 50 µl) contained: 5 µl 10 × Vent reaction buffer, 400 µM each dNTPs, 10 ng DNA template, 1 µM of each primer and 2 U of Vent polymerase (New England Biolab). The reactions were carried out for 20 cycles using a DNA thermal cycler (Ericomp Inc.). Each cycle included a heat denaturation step at 94 °C (1 min), followed by annealing of the primer at 50–55 °C (2 min) and primer extension at 72 °C (1–1.5 min). The above modification of existing protocols resulted in a high frequency of recovered deletion mutants. Products of PCR were analysed on 1.5–2% agarose gels after digestion with appropriate restriction enzymes. Small differences of 12 to 24 bp were readily observed in this system.

#### DNA procedures

Standard DNA techniques followed the protocols outlined by Sambrook *et al.* (1989). Plasmids were transformed into *P. aeruginosa* by the methods described by Olsen *et al.* (1982). All PCR fragments were sequenced to identify the specific deletions and to confirm that no errors were present in the PCR products. DNA sequencing utilized an Applied Biosystems automated fluorescence sequencer and dye terminator chemistry as detailed in ABI's protocols.

#### Characterization of the outer membrane

*E. coli* and *P. aeruginosa* outer membranes were isolated as described by Hancock and Carey (1979). SDS-PAGE utilized 8–11% acrylamide gels as described by Hancock and Carey (1979). Western immunoblotting utilized the techniques of Mutharia and Hancock (1985), and anti-OprD polyclonal antibody was prepared and purified according to the protocol of Siehnel *et al.* (1990).

#### Trypsinization studies

OprD variants in *P. aeruginosa* outer-membrane samples were digested using trypsin (TPCK treated, Sigma) at a concentration of 1 mg ml<sup>-1</sup>, in 10 mM Tris-HCl pH 8.0 at 37 °C for 1 h. Untreated samples were incubated in the same conditions except that trypsin was omitted. Proteolysis was stopped by heating at 90 °C for 10 min in solubilization-reduction mix (Hancock and Carey, 1979). The trypsinized samples were run on SDS-PAGE and analysed by Western immunoblot with anti-OprD polyclonal antibody.

#### Acknowledgements

This research was performed with the assistance of grants from the Medical Research Council of Canada and the Canadian Cystic Fibrosis Foundation (CCFF). H. Huang is the recipient of a CCFF Studentship.

#### References

- Agterberg, M., Adriaanse, H., Tijhaar, E., Resink, A., and Tommassen, J. (1989) Role of the cell surface-exposed regions of outer membrane protein PhoE of *Escherichia coli* K-12 in the biogenesis of the protein. *Eur J Biochem* **185**: 365–370.
- Benson, S.A., Occi, J.L.L., and Sampson, B.A. (1988) Mutations that alter the pore function of the OmpF porin of *Escherichia coli* K-12. *J Mol Biol* **203**: 961–970.
- Bollivar, D.W., and Bauer, C.E. (1992) Association of tetrapyrrole intermediates in the bacteriochlorophyll a biosynthetic pathway with the major outer-membrane porin protein of *Rhodobacter capsulatus*. *Biochem J* **282**: 471–476.
- Bosch, D., and Tommassen, J. (1987) Effects of linker insertions on the biogenesis and functioning of the *Escherichia coli* outer membrane pore protein PhoE. *Mol Gen Genet* **208**: 485–489.
- Bosch, D., Voorhout, W., and Tommassen, J. (1988) Export and localization of N-terminally truncated derivatives of *Escherichia coli* K-12 outer membrane protein PhoE. *J Biol Chem* **263**: 9952–9957.
- Bosch, D., Scholten, M., Verhagen, C., and Tommassen, J. (1989) The role of carboxy-terminal membrane-spanning fragment in the biogenesis of *Escherichia coli* K-12 outer membrane protein PhoE. *Mol Gen Genet* **216**: 144–148.
- Boulain, J.C., Charbit, A., and Hofnung, M. (1986) Mutagenesis by random linker insertion into the *lamB* gene of *Escherichia coli* K-12. *Mol Gen Genet* **205**: 339–348.
- Cornette, J.L., Cease, K.B., Margalit, H., Spouge, J.L., Berzofsky, J.A., and Delisi, C. (1987) Hydrophobicity scales and computational techniques for detecting amphipathic structures in proteins. *J Mol Biol* **195**: 659–685.
- Cowan, S.W., Schirmer, T., Rummel, G., Steiert, M., Ghosh, R., Pauptit, R.A., Jansonius, J., and Rosenbusch, J.P. (1992) Crystal structures explain functional properties of two *E. coli* porins. *Nature* **358**: 727–733.
- Devereux, J., Haerberli, P., and Smithies, O. (1984) A comprehensive set of sequence analysis programs for the VAX. *Nucl Acids Res* **12**: 387–395.



- Eisenberg, D., Weiss, R.M., and Terwilliger, T.C. (1982) The helical hydrophobic moment: a measure of the amphiphilicity of a helix. *Nature* **299**: 371–374.
- Fukuoka, T., Masuda, N., Takenouchi, T., Sekine, N., Iijima, M., and Ohya, S. (1991) Increase in susceptibility of *Pseudomonas aeruginosa* to carbapenem antibiotics in low-amino-acid media. *Antimicrob Ag Chemother* **35**: 529–532.
- Hancock, R.E.W. (1987) Role of porins in the outer membrane permeability. *J Bacteriol* **169**: 929–933.
- Hancock, R.E.W., and Carey, A.M. (1979) Outer membrane of *Pseudomonas aeruginosa*: heat- and 2-mercaptoethanol-modifiable proteins. *J Bacteriol* **140**: 902–910.
- Ho, S.N., Hunt, H.D., Horton, R.M., Pullen, J.K., and Pease, L.R. (1989) Site-directed mutagenesis by overlap extension using the polymerase chain reaction. *Gene* **77**: 51–59.
- Huang, H., and Hancock, R.E.W. (1993) Genetic definition of the substrate selectivity of outer membrane porin protein OprD of *Pseudomonas aeruginosa*. *J Bacteriol* **175**: 7793–7800.
- Huang, H., Siehnel, R., Bellido, F., Rawling, E., and Hancock, R.E.W. (1992) Analysis of two gene regions involved in the expression of the imipenem-specific, outer membrane porin protein OprD of *Pseudomonas aeruginosa*. *FEMS Microbiol Lett* **97**: 267–274.
- Jeanteur, D., Lakey, J.H., and Pattus, F. (1991) The bacterial porin superfamily: sequence alignment and structure prediction. *Mol Microbiol* **5**: 2153–2164.
- Jeanteur, D., Lakey, J.H., and Pattus, F. (1994) The porin superfamily: diversity and common features. In *The Bacterial Cell Wall*, Ch. 17. Ghuyssen, J.M., and Hakenbeck, R. (eds). Amsterdam: Elsevier Science, pp. 363–380.
- Kreusch, A., Neubuser, A., Schiltz, E., Weckesser, J., and Schulz, G.E. (1994) Structure of the membrane channel porin from *Rhodospseudomonas blastica* at 2.0 Å resolution. *Protein Sci* **3**: 58–63.
- van der Ley, P., Amesz, H., Tommassen, J., and Lugtenberg, B. (1985) Monoclonal antibodies directed against the cell surface-exposed part of PhoE pore protein of the *Escherichia coli* K-12 outer membrane. *Eur J Biochem* **147**: 401–407.
- Manoil, C., and Beckwith, J. (1986) A genetic approach in analysing membrane protein topology. *Science* **233**: 1403–1408.
- Misra, R., and Benson, S.A. (1988) Genetic identification of the pore domain of the OmpC porin of *Escherichia coli* K-12. *J Bacteriol* **170**: 3611–3617.
- Mutharika, L.M., and Hancock, R.E.W. (1985) Characterization of two surface-localized antigenic sites on porin protein F of *Pseudomonas aeruginosa*. *Can J Microbiol* **31**: 381–386.
- Needleman, S.B., and Wunsch, C.D. (1970) A general method applicable to the research for similarities in the amino acid sequence of two proteins. *J Mol Biol* **48**: 443–453.
- Olsen, R.H., DeBusscher, W., and McCombie, W.R. (1982) Development of broad host range vectors and gene banks: self-cloning of the *Pseudomonas aeruginosa* PAO chromosome. *J Bacteriol* **150**: 60–69.
- Paul, C., and Rosenbusch, J.P. (1985) Folding patterns of porin and bacteriorhodopsin. *EMBO J* **4**: 1593–1597.
- Saiki, R.K., Scharf, S., Faloona, F., Mullis, K.B., Horn, G.T., Erlich, H.A., and Arnheim, N. (1985) Enzymatic amplification of  $\beta$ -globin genomic sequences and restriction site analysis for diagnosis of sickle cell anemia. *Science* **230**: 1350–1354.
- Sambrook, J., Fritsch, E.F., and Maniatis, T. (1989) *Molecular Cloning: A Laboratory Manual*, 2nd edn. Cold Spring Harbor, New York: Cold Spring Harbor Laboratory Press.
- Schulein, K., Schmid, K., and Benz, R. (1991) The sugar-specific outer membrane channel ScrY contains functional characteristics of general diffusion pores and substrate-specific porins. *Mol Microbiol* **5**: 2233–2241.
- Schulz, G.E. (1994) Structure–function relationships in porins as derived from a 1.8 Å resolution crystal structure. In *The Bacterial Cell Wall*, Ch. 15. Ghuyssen, J.M., and Hakenbeck, R. (eds). Amsterdam: Elsevier Science, pp. 343–352.
- Schweizer, H.P. (1991) Cloning vector for *Escherichia-Pseudomonas* cloning derived from pUC18/19. *Gene* **97**: 109–112.
- Siehnel, R., Martin, N.L., Hancock, R.E.W. (1990) Sequence and relatedness in other bacteria of the *Pseudomonas aeruginosa* oprP gene coding for the phosphate-specific porin P. *Mol Microbiol* **4**: 831–838.
- Trias, J., and Nikaido, H. (1990a) Protein D2 channel of the *Pseudomonas aeruginosa* outer membrane has a binding site for basic amino acids and peptides. *J Biol Chem* **265**: 15680–15684.
- Trias, J., and Nikaido, H. (1990b) Outer membrane protein D2 catalyzes facilitated diffusion of carbapenem and penem through the outer membrane of *Pseudomonas aeruginosa*. *Antimicrob Ag Chemother* **34**: 52–57.
- Vallette, F., Mege, E., Reiss, A., and Adesnik, M. (1989) Construction of mutant and chimeric genes using the polymerase chain reaction. *Nucl Acids Res* **17**: 723–733.
- Vogel, H., and Jahnig, F. (1986) Models for the structure of outer membrane proteins of *Escherichia coli* derived from Raman spectroscopy and prediction methods. *J Mol Biol* **190**: 191–199.
- Weiss, M.S., and Schulz, G.E. (1992) Structure of porin refined at 1.8 Å resolution. *J Mol Biol* **227**: 493–509.
- Wong, S.Y., Jost, H., and Hancock, R.E.W. (1993) Linker-insertion mutagenesis of *Pseudomonas aeruginosa* outer membrane protein OprF. *Mol Microbiol* **10**: 283–292.
- Woodruff, W.A. and Hancock, R.E.W. (1988) Construction and characterization of *Pseudomonas aeruginosa* protein F-deficient mutants after in vivo and in vitro insertion mutagenesis of the cloned gene. *J Bacteriol* **170**: 2592–2598.

Copyright of Molecular Microbiology is the property of Blackwell Publishing Limited and its content may not be copied or emailed to multiple sites or posted to a listserv without the copyright holder's express written permission. However, users may print, download, or email articles for individual use.